Fuel 278 (2020) 118216

Contents lists available at ScienceDirect

Fuel

journal homepage: www.elsevier.com/locate/fuel

Full Length Article

Combustion stability analysis for non-standard low-calorific gases: Blast furnace gas and coke oven gas

Long Zhang[a], Wenwen Xie[a], Zhuyin Ren[a,b,*]

[a] School of Aerospace Engineering, Tsinghua University, Beijing 100084, China
[b] Institute for Aero Engine, Tsinghua University, Beijing 100084, China

ARTICLE INFO

Keywords:
Non-standard low-calorific value gas
Combustion stability
Fuel switching
PSR
CEMA

ABSTRACT

The effective and efficient utilization of byproduct fuels has gained increasing attention in all industrial fields. In this study, flame stabilization mechanisms for non-standard low-calorific value (NLCV) gases of blast furnace gas and coke oven gas have been systematically analyzed under practical operating conditions of hot air heaters. The complex oscillatory dynamics has been successfully reproduced with the unsteady perfectly stirred reactor combustion model. The differences in the combustion stabilities between NLCV gases have been further revealed, with the kinetic importance of individual variable and chemical reaction for the complex dynamics being quantified with chemical explosive mode analysis. Then the effects of gas composition and fuel blending on combustion instability are investigated. The optimal fuel switching temperature, switching schemes and oscillating combustion inhibition methods are finally proposed for stable combustion of blast furnace gas and coke oven gas. The tolerance range of flow rate fluctuations are increased by 10% and 30% with selecting fuel switching scheme and initial combustion state reasonably.

1. Introduction

With the threat of global energy crisis and environmental effects of global warming, the effective and efficient utilization of byproduct fuels has gained increasing attention in all industrial fields. In the process of non-standard manufacturing industries such as steel mills and chemical plants, non-standard fuel gases with complex components are produced, such as blast furnace gas, coke oven gas, converter gas, analytical gas, etc. [1–3] These non-standard fuel gases mainly consist of H_2, CO and C1-C4 hydrocarbon in different ratios. Only coke oven gas, which has half the calorific value of NG as about 4.75 kWh/m^3, can be directly ignited at a normal temperature [4–5], while the other non-standard fuel gases, e.g., blast furnace gas with one-tenth the calorific value of NG as about 0.95 kWh/m^3, need to be burnt at a high ambient temperature due to low calorific value [6–8]. Currently industrial combustion devices such as hot air heater, built-in combustion chamber, offset flame burner, etc. have been developed for in situ combustion of non-standard fuel gases. Among them, hot air heater is most widely used for burning blast furnace gas and coke oven gas. NLCV gases are prone to combustion instability especially for blast furnace gas and coke oven gas [9–11], which pose great challenge for reliable industrial operation. For example, oscillating combustion in the hot air heater may occur at high ambient temperatures, which causes the vibration of the heater body and the instability of the outlet parameters. Furthermore, extinction occasionally occurs since the switching temperature, determined mainly based on experience in practice, is not readily known and may not be optimal during fuel switching stage.

Extensive studies have been performed on the combustion characteristics of NLCV gases, from the perspective of chemical kinetics [12–14], and experimental and modeling studies in practical combustion devices [15–17]. Fischer et al. [18] investigated the accuracy of existing detailed mechanisms for predicting ignition delay times of mixtures containing methane, hydrogen, carbon monoxide and carbon dioxide. Results showed that the kinetic modeling of NLCV gases is subject to further improvement. Experimental studies have been performed to investigate the combustible limit and emission performance [19–22]. Ortiz-Imedio [23] studied the engine performance and emissions of pure hydrogen, carbon monoxide and coke oven gas in stationary internal combustion engines, and results showed that coke oven gas produces less NO_x, HC, CO and CO_2 emissions indicating coke oven gas as a good fuel for internal combustion engines. More importantly, several methods have been investigated to enhance the combustion stability of NLCV gases [4–6]. In [6], reactant preheating is proposed to increase the combustion stability through large-scale experiments. The operational range is extended, while CO and NO_x emissions are less than 20 ppm even when reactants are preheated. Among various

* Corresponding author at: School of Aerospace Engineering, Tsinghua University, Beijing 100084, China.
E-mail address: zhuyinren@tsinghua.edu.cn (Z. Ren).

https://doi.org/10.1016/j.fuel.2020.118216
Received 20 March 2020; Received in revised form 30 April 2020; Accepted 25 May 2020

numerical studies on combustion of NLCV gases [24–26], He et al [26] established a numerical model to analyze the combustion characteristics of coke oven gas in a porous media burner and showed that the stability of the flame is closely related to the ignition position and the length of the preheating zone.

Most of the existing researches focus on the chemical kinetics of NLCV gases or the applications of NLCV gases in specific burners. There are few studies on oscillating combustion in reactors resulting from periodic extinction and reignition governed by the subtle mixing-chemical kinetics interaction or due to the inflowing flow rate fluctuation under industrial conditions. Consequently, during the use of specific equipment, e.g., a hot air heater, the choice of fuel switching temperature lacks of theoretical foundation. The mechanism of oscillating combustion, the effects of fuel switching scheme and flow rate fluctuation on combustion characteristics remain to be studied.

In this study, a detailed analysis of flame stabilization mechanisms for NLCV gases burning in a hot air heater has been performed. The complex oscillatory dynamics has been successfully reproduced with the unsteady perfectly stirred reactor (PSR) combustion model together with GRI-MECH 3.0 mechanism [27]. The differences in the combustion stabilities between NLCV gases have been further revealed with the chemical explosive mode analysis (CEMA), which quantifies the kinetic importance of individual variable and chemical reaction for the complex dynamics observed in practical operations. The flame stabilization mechanisms under different conditions of industrial practice are then revealed, and the optimal fuel switching temperature, switching schemes and oscillating combustion inhibition methods are proposed for stable combustion in the hot air heater.

The remainder of this paper is organized as follows. In Section 2, the hot air heater is introduced, followed by the descriptions of the unsteady PSR model and the CEMA method. In Section 3, the complex combustion characteristics of blast furnace gas and coke oven gas under different gas compositions, fuel switching schemes and flow rate fluctuations are analyzed in details and validated against the experimental data. Conclusions are drawn in Section 4.

2. Methodology

2.1. Hot air heater

Hot air heater is an in-situ combustion equipment, and mainly used for NLCV gas combustion in steel mills and chemical plants. Fig. 1 shows the schematic diagram of the hot air heater model. The wall of heater body is composed of heavy refractory brick layer, light refractory brick layer, aluminum silicate layer and metal layer from inside to outside. The four thermal insulation layers can reduce the heat loss and realize high ambient temperature within the heater. The burner has separate inlets for each fuel gas and air, and mixes fuel gas and air at the burner outlet by reverse swirlers to form a recirculation zone for stable combustion inside the heater body.

During the operation of a hot air heater, two types of fuel gases are required. The first gas needs to be ignited at normal temperature, and is generally coke oven gas. The second gas needs to be burnt at a high ambient temperature, and is generally blast furnace gas. The work flow of hot air heater can be divided into three stages: ignition stage, fuel switching stage and final combustion stage. During the ignition stage, coke oven gas is ignited at normal temperature and burnt to increase the ambient temperature in the heater. Fuel switching stage starts when the ambient temperature exceeds the switching temperature under which blast furnace gas can be burnt steadily, and coke oven gas is gradually replaced by blast furnace gas in this stage. After fuel switching, blast furnace gas is burnt independently during the final combustion stage. Hot air heater has different types of combustion instabilities in different stages, including oscillating combustion in the ignition stage, switching instability in the fuel switching stage and fuel gas fluctuations both in the fuel switching stage and final combustion stage.

Table 1
Typical fuel compositions of coke oven gas and blast furnace gas (volume fraction).

Fuel composition	H2	CO	CH4	N2	
Coke oven gas	COG_1	50.0%	9.0%	30.0%	11.0%
	COG_2	60.0%	9.0%	25.0%	6.0%
	COG_3	70.0%	9.0%	20.0%	1.0%
	COG_4	50.0%	14.0%	30.0%	6.0%
	COG_5	50.0%	19.0%	30.0%	1.0%
Blast furnace gas	BFG_1	2.5%	22.5%	0.0%	75.0%
	BFG_2	1.0%	24.0%	0.0%	75.0%
	BFG_3	5.0%	20.0%	0.0%	75.0%

The typical fuel compositions of coke oven gas and blast furnace gas are shown in Table 1 within the data range of [2] and [4]. The equivalent ratio and mixing ratio in the following study are calculated based on the fuel compositions in Table 1. All the experimental data, including system temperature, burning state, oscillating state and fluctuations, are from the field tests of No. 3 hot air heater in Shiheng steel plant of China. From industrial gas analysis data, the typical gas compositions of coke oven gas and blast furnace gas burned in this hot air heater are COG_1 and BFG_1 in Table 1. Each field test is an independent test including the pre-purge, ignition, fuel switching, load adjustment and extinction processes. During the field tests, the effects of the changes in fuel composition, equivalent ratio, ambient temperature and other relevant parameters were tested. The flow rate of blast furnace gas fluctuates due to the change of upstream process parameters.

2.2. Unsteady perfectly stirred reactor model

The combustion of $H_2/CO/CH_4/O_2/N_2$ mixtures representing non-standard fuel gases is investigated in a nonadiabatic unsteady PSR to reveal the complex dynamics exhibited in industrial hot air heaters. The

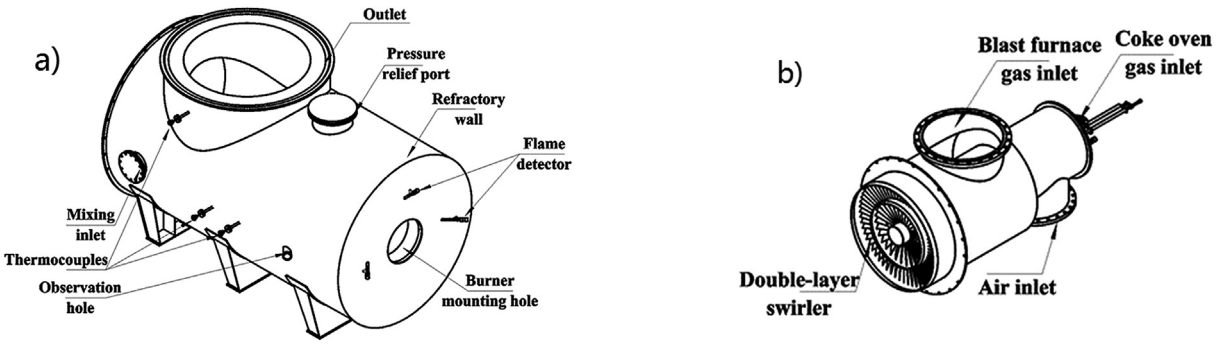

Fig. 1. Schematic diagram of hot air heater. (a) heater body; (b) burner.

typical operating characteristics of hot air heater, e.g., constant volume, constant pressure and high mixing level, are consistent with the assumptions in an ideal PSR model. Unsteady PSRs have been demonstrated for reproducing complex oscillatory dynamics in the H_2/CO/CH_4 combustion [28–32]. The detailed mechanism employed is GRI-MECH 3.0 [27], which involves 53 species and 325 reactions. It is worth mentioning that GRI-MECH 3.0 for kinetic modeling of NLCV gases may be subject to further improvement, especially for the ignition and extinction conditions. It is used as a first attempt to test if one can reproduce the complex combustion dynamics observed in field tests and it has been also employed for the gases with similar compositions in [6] and [18].

The hot air heater in this study operates under constant atmospheric pressure. The heater chamber is cylindrical with the constant volume of 13.82 m^3. The mass flow rate of the inflowing mixture is 2.75 kg/s at 300 K, and the residence time is about 1.0 s calculated according to

$$\tau_{res} = \frac{\rho V}{m_a}, \tag{1}$$

where τ_{res} is the residence time, ρ is the density of the mixture in the reactor, V is the volume of hot air heater, and m_a is the mass flow rate of the inflowing mixture. With the assumption of perfect mixing in the reactor, the dynamics can be modeled by a nonadiabatic PSR governed by the following set of ordinary differential equations (ODEs),

$$\frac{d\boldsymbol{Y}}{dt} = \frac{\boldsymbol{Y_{in}} - \boldsymbol{Y}}{\tau_{res}} + \boldsymbol{S} \tag{2}$$

$$\frac{dT}{dt} = \frac{\sum_i q_i R_i}{\rho C_p} - \frac{T - T_{in}}{\tau_{res}} - \frac{Q_{loss}(T - T_a)}{\rho C_p} \tag{3}$$

where Y_{in} and T_{in} are the species mass fraction and temperature of the inflowing stream, T_a is the ambient temperature, $Q_{loss}$is the heat loss coefficient, T is the mixture temperature, C_p is the specific heat of the mixture in the reactor, $R_i$is the ith reaction rate, $q_i$is the exothermicity of the ith reaction, and the vector S determined by chemical kinetics is the rate of change of the composition due to chemical reactions.

The combustion characteristics of PSR is determined by the parameters ofτ_{res}, Y_{in}, T_{in}, P, T_a and Q_{loss}, together with the initial conditions. According to the operating conditions of the hot air heater considered, P = 101325 Pa, T_{in} = 300K, Q_{loss}=4$JK^{-1}m^{-3}s^{-1}$, and τ_{res}=1.0 s for both coke oven gas and blast furnace gas. Note that the heat loss coefficient Q_{loss} is obtained by calculating the equivalent thermal resistance of the heater wall. The initial conditions of the PSR are the adiabatic and isobaric chemical-equilibrium state of the inflowing mixture. Eq. (2–3) are numerically integrated with the ODE solver DDASAC [33].

2.3. Chemical explosive mode analysis

The chemical explosive mode analysis (CEMA) [34–36] is developed based on eigen-analysis as a systematic diagnostic of critical flame features, and is promising in resolving the complex physiochemical couplings between flow and chemical kinetics. The CEMA method analyzes key flame features through the eigenvalue decomposition of local chemical Jacobian, where the chemical explosive modes (CEMs) are detected by the real parts of eigenvalues and flame stabilization mechanisms are identified through the explosion index (EI) [34–35] and the participation index (PI) [36]. The existence of a CEM indicates a mixture that is explosive in nature. The growth of small perturbations tends to increase exponentially along the direction of the eigenvector associated with the CEM if the mixture is isolated [34]. CEMs have been found to be important for the local extinction and reignition processes of combustion problems.

In this study, the CEMA method is used to analyze if there exist explosive mixtures for the observed oscillatory combustion, and if so what are the key species and reactions. This may shed lights on the key physics during the complex oscillatory combustion. Considering that the residence time of hot air heater, e.g., 1.0 s is much larger than the timescale of the possible CEM, it is convenient to perform CEMA analysis and analyze some key dynamic features of the unsteady PSR based on the evolution of the local composition due to chemical reaction, i.e.,

$$\frac{d\boldsymbol{c}}{dt} = \boldsymbol{\omega}(\boldsymbol{c}) \tag{4}$$

where c is the vector of dependent variables consisting of species molar concentrations and temperature, and $\boldsymbol{\omega}$ is the chemical source term. The chemical Jacobian of the RHS of Eq. (4) is given by

$$J_\omega = \frac{\partial \omega(c)}{\partial c}. \tag{5}$$

The local chemical information is fully encoded in the Jacobian matrix, J_ω, of the chemical source term, $\boldsymbol{\omega}$. An eigenmode of J_ω, including an eigenvalue and a corresponding pair of left and right eigenvectors, defines a chemical mode. A chemical mode is further defined as a CEM if the real part of the associated eigenvalue, $\hat{\lambda}_e$, is positive [34]. The eigenvalue $\hat{\lambda}_e$ and chemical Jacobian J_ω are related by

$$\lambda_e = \boldsymbol{b_e} \cdot \boldsymbol{J_\omega} \cdot \boldsymbol{a_e}, \tag{5}$$

where b_e and a_e are left and right eigenvectors, respectively, associated with the CEM.

The contribution of a chemical species to a CEM is quantified by the explosion index (EI) [34–35],

$$EI = \frac{diag|\boldsymbol{a_e}\boldsymbol{b_e}|}{sum(diag|\boldsymbol{a_e}\boldsymbol{b_e}|)} \tag{6}$$

where "||" denotes the element-wise absolute values. EI is a normalized vector with each value lying within [0, 1]. A large value close to unity indicates that the ith variable, a species or temperature, is dominant in the CEM.

The contribution of a reaction to the CEM is quantified by the participation index (PI) [36],

$$PI = \frac{(|(b_e \cdot W) \otimes R|)}{sum(|(b_e \cdot W) \otimes R|)} \tag{7}$$

where W is the stoichiometric coefficient matrix, R is the vector of net rates for the reactions, "⊗" denotes the element-wise multiplication of two vectors. Each value in PI is also normalized to [0, 1]. If the ith value is close to unity, the ith reaction is dominant in the CEM. CEMA is next applied as a computational diagnostic for the combustion of NLCV gases. All the EIs and PIs for each dependent variable and reaction are calculated and reordered in descending order. The variables and reactions corresponding to the large values of EIs and PIs are considered as the dominant factors of CEM in the following sections.

3. Results and discussions

3.1. Combustion characteristics of blast furnace gas and coke oven gas

3.1.1. Combustion dynamics: burning state and oscillation

Fig. 2 shows the temperature evolution during the independent combustion process at representative thermal conditions. The initial temperature in the reactor is raised to chemical-equilibrium temperature. For burnt cases of blast furnace gas BFG_1 as shown in Fig. 2a, temperature gradually decreases towards the final operating temperature. The final operating temperature decreases from 1480 K in the adiabatic case to 1040 K in the case of heat loss with T_a = 873 K. This suggests that the combustion intensity of blast furnace gas decreases with decreasing ambient temperature. When the ambient temperature reaches a critical temperature, the heat loss of the system exceeds combustion heat release and extinction occurs. Low-calorific gas has a critical ambient temperature corresponding to its calorific value, and this critical ambient temperature is the lowest fuel switching

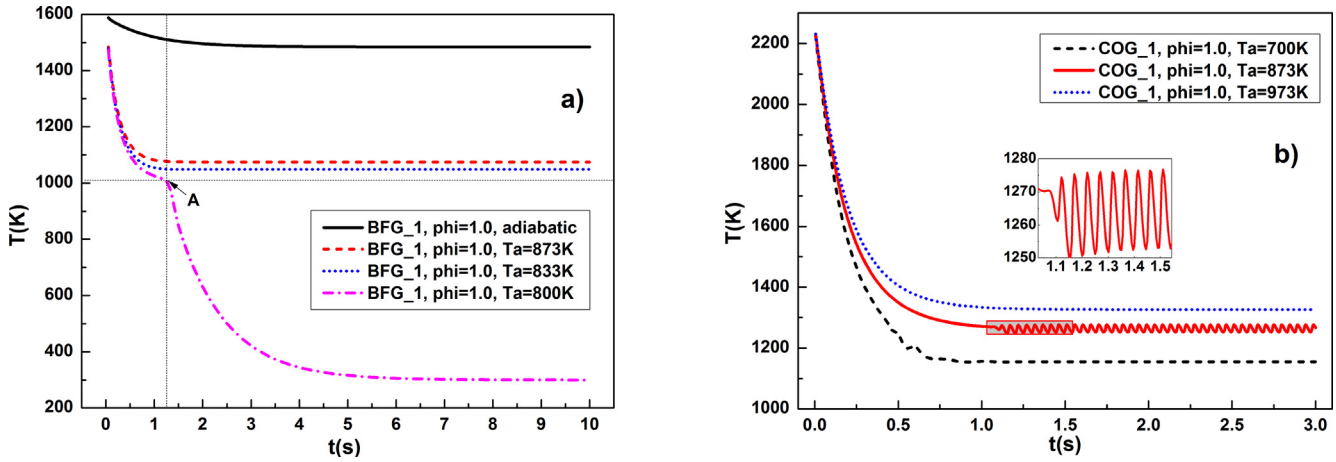

Fig. 2. Temperature evolution from the combustion process of burning blast furnace gas and coke oven gas, respectively. (a) BFG_1, phi = 1.0; (b) COG_1, phi = 1.0.

temperature at specified fuel composition and equivalent ratio. The critical ambient temperature for blast furnace gas of BFG_1 with phi = 1.0 is around 800 K. For the unburnt case demonstrated, temperature decreases rapidly to the inflowing temperature following a slow drop to the inflection-point (Point A) temperature.

Fig. 2b shows the temperature evolution for the case (COG_1, phi = 1.0) at different ambient temperatures. As shown, the final operating temperature of coke oven gas (1262 K) is about 220 K higher than that of blast furnace gas (1040 K) due to the difference in the calorific value. With decreasing ambient temperature, the final operating temperature of coke oven gas decreases from 1326 K at T_a = 973 K to 1155 K at T_a = 700 K, and no extinction occurs. More importantly, for coke oven gas, in a specific ambient temperature range, the temperate oscillates and the flame becomes unstable, which could lead to severe operating safety issue. As shown, at T_a = 873 K, temperature oscillates periodically with a frequency of around 20 Hz and an amplitude of 28 K.

Fig. 3 shows the temperature oscillating ranges for the case (COG_1, phi = 1.0) at different ambient temperatures. With increasing ambient temperature from 760 K to 900 K, the mean temperature increases gradually from 1201 K to 1282 K, and the temperature oscillating ranges decrease from 54 K (between 1174 K and 1228 K) to 10 K (between 1277 K and 1287 K). This suggests that coke oven gas with higher ambient temperature can be burnt more steadily. The measured temperature range from field test is from 1224 K to 1231 K when T_a = 800 K, and from 1255 K to 1259 K when T_a = 873 K. As shown, the model results agree qualitatively with the experimental data and the unsteady PSR model is adequate to reveal the key dynamic features, although the accuracy in the oscillatory temperature range is subject to further improvement.

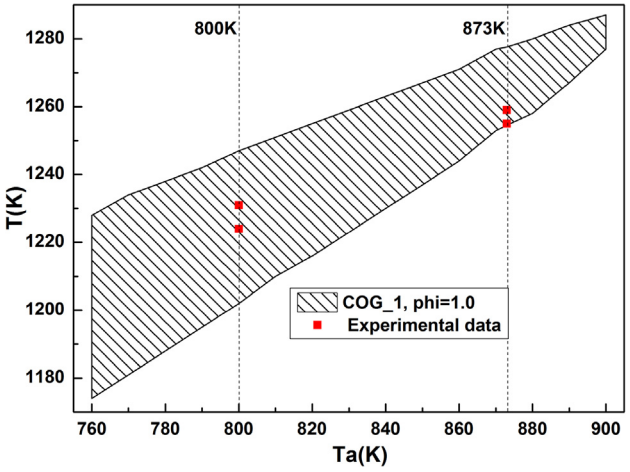

Fig. 3. Temperature oscillating ranges for the case (COG_1, phi = 1.0) at different ambient temperatures. Red squares: experimental data; upper boundary of shaded area: the highest oscillating temperature; lower boundary of shaded area: the lowest oscillating temperature. (For interpretation of the references to colour in this figure legend, the reader is referred to the web version of this article.)

3.1.2. Kinetic importance of individual variable and chemical reaction

Fig. 4 shows CEMA analysis for the unburnt case (BFG_1, phi = 1.0, T_a = 800 K) near the inflection point (Point A) in Fig. 4a. Fig. 4b shows the values of $\mathrm{sign}[\mathrm{Re}(\Lambda_e)]\cdot\lg(1+|\mathrm{Re}(\Lambda_e)|)$, where Λ_e is the largest non-zero eigenvalue of the Jacobian matrix J_ω and $\mathrm{Re}(\Lambda_e)$represents the real part of Λ_e. Note that sign stands for the signum function, and lg is the base 10 logarithm of a number. The values of $\mathrm{sign}[\mathrm{Re}(\Lambda_e)]\cdot\lg(1+|\mathrm{Re}(\Lambda_e)|)$implies the states of the solutions on the profile, where negative, positive but around zero, and positive with large value indicate the burnt, unburnt and explosive state respectively. The transition between ignition and extinction occurs when the value crosses zero.

As shown in Fig. 4b, only one zero-crossing point (Point B) occurs during the whole process, indicating that extinction occurs at Point B and no reignition happens subsequently. In addition temperature evolves as a two-stage drop with the inflection point (Point A). Around point A, the state transitions quickly from the explosive state to the unburnt state. Fig. 4c shows the explosive indices (EIs) and the participation index (PI) of R36 (H+ O_2 + N_2 ⇔ HO_2 + N_2). Temperature

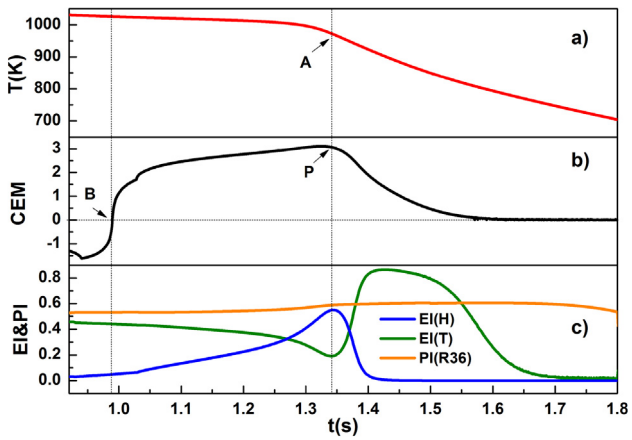

Fig. 4. CEMA analysis for the unburnt case (BFG_1, phi = 1.0, Ta = 800 K). (a) temperature evolution; (b) the values of $\mathrm{sign}[\mathrm{Re}(\Lambda_e)]\cdot\lg(1+|\mathrm{Re}(\Lambda_e)|)$; (c) EI(H), EI(T) and PI(R36: H+ O_2 + N_2 ⇔ HO_2 + N_2).

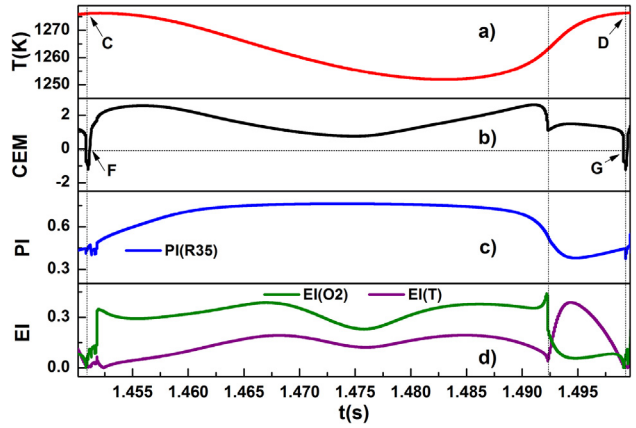

Fig. 5. CEMA analysis for the single oscillating period of the case (COG_1, phi = 1.0, Ta = 873 K). (a) temperature evolution; (b) the values of $\mathrm{sign}[\mathrm{Re}(\Lambda_e)]\cdot\lg(1+|\mathrm{Re}(\Lambda_e)|)$; (c) PI(R35: H+ O_2 + H_2 O⇔ HO_2 + H_2O); (d) EI(O_2) and EI(T).

and radical H are the important variables during the transition among the different states. In addition, the key reaction for the extinction process is R36 (H+ O_2 + N_2 ⇔ HO_2 + N_2) which indicates that radical H is crucial to the extinction process.

One single oscillating period of the case (COG_1, phi = 1.0, T_a = 873 K) is analyzed in Fig. 5 with CEMA. Fig. 5a shows the sinusoidal temperature evolution within one single oscillating period from the start point (Point C) to the end point (Point D). The two zero-crossing points (Point F and Point G) in Fig. 5b indicates that extinction and ignition occur sequentially within the single oscillating period. The system is only in the burnt state near the start and end of the period, and transitions into the explosive state from Point F to Point G. Species O_2 and temperature play the important role in the different explosive states with the key reaction R35 (H+ O_2 + H_2 O⇔ HO_2 + H_2O). Before ignition, temperature dominates the CEM to indicate that radical pool is built up for chemical reactions. The periodic extinction and reignition processes under the influence of chemical reactions lead to periodic changes in the thermal balance between heat release and heat loss, resulting in the oscillating combustion of coke oven gas.

3.2. Effects of gas composition on combustion characteristics

3.2.1. Blast furnace gas

The effects of gas compositions of blast furnace gas on system burning state are shown in Fig. 6. When hydrogen content increases from 1% (BFG_2) to 2.5% (BFG_1) and 5% (BFG_3), the lowest ambient temperature that can sustain burnt state decreases from 840 K to 805 K and 790 K. This suggests that blast furnace gas with higher hydrogen content can be ignited more easily, since hydrogen is chemically more active than carbon monoxide. The experimental data from industrial field tests under different ambient temperatures (800 K, 843 K and 873 K) are shown by red squares in Fig. 6. As shown, the model results agree well with the experimental data.

3.2.2. Coke oven gas

The effects of coke oven gas compositions on oscillating combustion are demonstrated in Fig. 7 for the cases of COG_1, COG_2, COG_3, COG_4 and COG_5. It is observed that the contents of hydrogen and carbon monoxide have dramatically different impacts on the ambient temperature range for oscillating combustion of coke oven gas. When hydrogen content increases from 50% (COG_1) to 60% (COG_2) and 70% (COG_3), the ambient temperature range for oscillating combustion narrows from 140 K (between 760 K and 900 K) to 90 K (between 770 K and 860 K) and 60 K (between 750 K and 810 K), and the highest ambient temperature for oscillating combustion decreases from 900 K

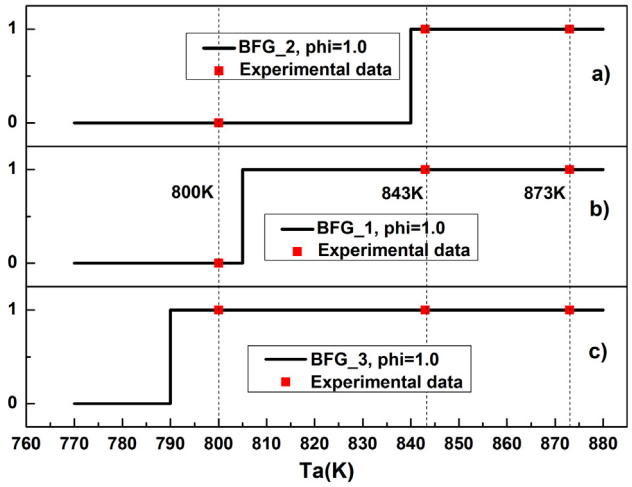

Fig. 6. Effects of blast furnace gas compositions on system burning state. (a) BFG_2; (b) BFG_1; (c) BFG_3. Key: red squares, experimental data; 1, burnt; 0, unburnt. (For interpretation of the references to colour in this figure legend, the reader is referred to the web version of this article.)

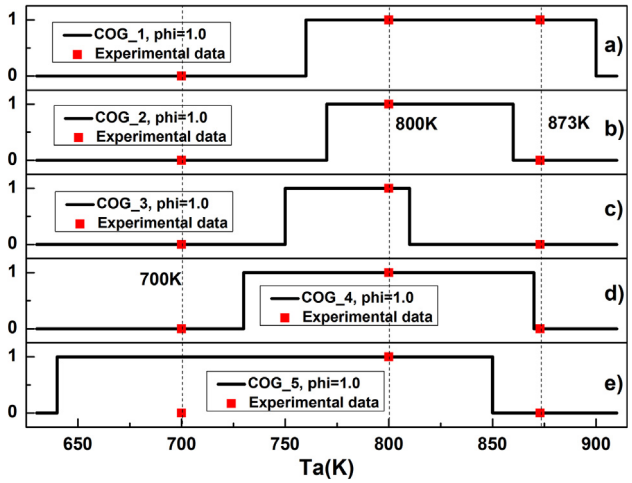

Fig. 7. Effects of coke oven gas compositions on oscillating combustion. (a) COG_1; (b) COG_2; (c) COG_3; (d) COG_4; (e) COG_5. Key: red squares, experimental data; 1, oscillating combustion; 0, stable combustion. (For interpretation of the references to colour in this figure legend, the reader is referred to the web version of this article.)

to 860 K and 810 K. In contrast, when carbon monoxide content increases from 9% (COG_1) to 14% (COG_4) and 19% (COG_5), the ambient temperature range for oscillating combustion broadens from 140 K (between 760 K and 900 K) to 140 K (between 730 K and 870 K) and 190 K (between 640 K and 850 K), and the highest ambient temperature for oscillating combustion decreases from 900 K to 870 K and 850 K. This suggests that coke oven gas with higher hydrogen content or lower carbon monoxide content have narrow ambient temperature range for oscillating combustion and can be burnt more steadily. Field tests have been carried out at different ambient temperatures (700 K, 800 K and 873 K) for coke oven gas combustion, and the experimental data in Fig. 7 validate the model results.

3.2.3. Blends of blast furnace gas and coke oven gas

During industrial operation, hot air heater can be fed by the blends of blast furnace gas and coke oven gas to modulate the combustion characteristics of the system. Fig. 8 illustrates the influence of mixing ratio, i.e., the volume fraction of blast furnace gas in the blended mixture, on oscillating combustion. It is observed that temperature

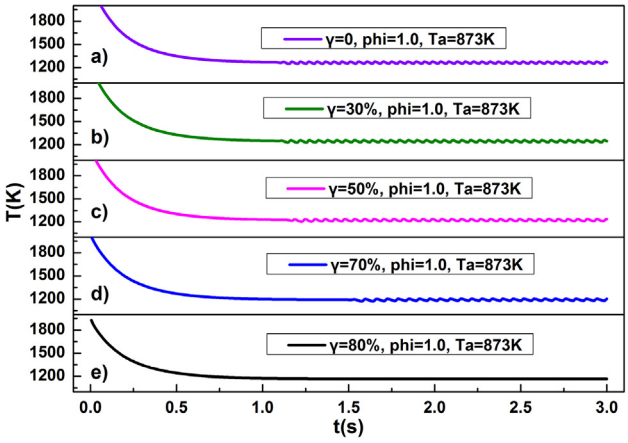

Fig. 8. Effects of mixing ratio γ on oscillating combustion with phi = 1.0, Ta = 873 K. (a) γ = 0; (b) γ = 30%; (c) γ = 50%; (d) γ = 70%; (e) γ = 80%.

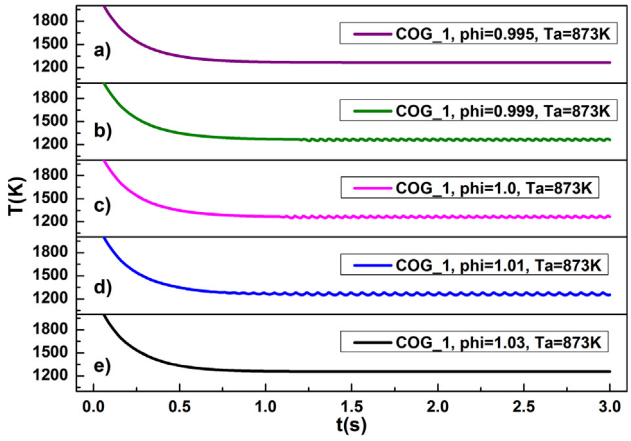

Fig. 10. Effects of equivalent ratio on oscillating combustion of coke oven gas. (a) phi = 0.995; (b) phi = 0.999; (c) phi = 1.0; (d) phi = 1.01; (e) phi = 1.03.

oscillating period increases and amplitude decreases with increasing fraction of blast furnace gas. But only when blast furnace gas reaches significant fraction, i.e., 80%, oscillating combustion disappears. This suggests that the blends of blast furnace gas and coke oven gas decreased the content of hydrogen which is chemically more active and the relevant rapid heat release reactions were inhibited. It made the heat balance between heat release and heat loss easier to achieve and the phenomenon of oscillating combustion was inhibited.

3.3. Effects of equivalent ratio on combustion characteristics

For blast furnace gas, the effects of equivalent ratios on system burning state are shown in Fig. 9. When equivalent ratio increases from 1.0 to 1.4, the lowest ambient temperature that can sustain burnt state first decreases from 805 K (phi = 1.0) to 755 K (phi = 1.1), but then increases to 775 K (phi = 1.2) and 825 K (phi = 1.4). This suggests that slight fuel rich is beneficial for stable combustion, but further increase in equivalent ratio has negative effect on stable combustion. The field test data with the above equivalent ratios at the ambient temperatures of 800 K, 843 K and 873 K are also shown in Fig. 9. As shown, the test data fall into the model prediction.

For coke oven gas, the effects of equivalent ratio on oscillating combustion are demonstrated in Fig. 10 for the cases of phi = 0.995, 0.999, 1.0, 1.01 and 1.03. It is observed that both temperature oscillating period and amplitude peak around the stoichiometry. But the oscillation is inhibited once it is slightly fuel lean or fuel rich equivalent ratio, i.e., phi less than 0.995 or phi > 1.03, due to the decrease of heat release intensity. This is consistent with the industrial practice of adopting fuel lean combustion to inhibit oscillating combustion of coke oven gas in the field.

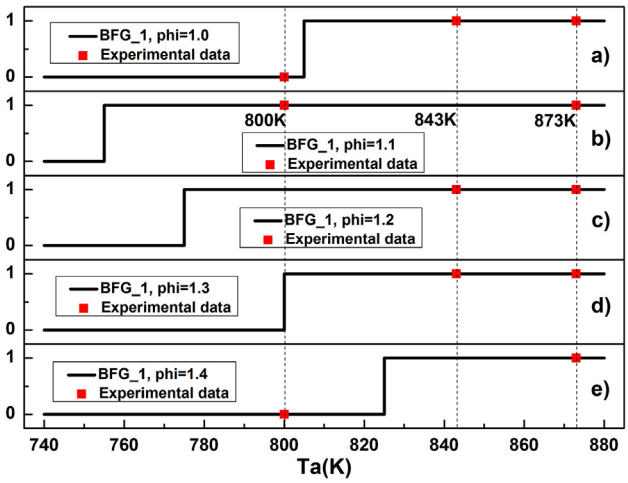

Fig. 9. Effects of equivalent ratios on system burning state of blast furnace gas. (a) phi = 1.0; (b) phi = 1.1; (c) phi = 1.2; (d) phi = 1.3; (e) phi = 1.4. Key: red squares, test data; 1, burnt; 0, unburnt. (For interpretation of the references to colour in this figure legend, the reader is referred to the web version of this article.)

3.4. Combustion characteristics during fuel switching stage

In industrial processes, the optimal fuel switching temperature is 873 K (T_a = 873 K) as shown in Fig. 2a, and the two initial states of coke oven gas before fuel switching are the stable combustion initial state (coke oven gas, phi = 0.95, T_a = 873 K) denoted as SCIS and the oscillating combustion initial state (coke oven gas, phi = 1.0, T_a = 873 K) denoted as OCIS. The frequency and amplitude of temperature oscillations in the OCIS state are 20 Hz and 28 K as shown in Fig. 2b.

3.4.1. Fuel switching schemes

Hot air heater has two fuel switching schemes. In scheme A, coke oven gas and blast furnace gas are switched in equal proportion according to the start and end time of fuel switching, denoted as SS = A. In scheme B, fuel switching has two stages. In the first stage, the inflowing calorific value remains unchanged until the flow rate of coke oven gas decreases to zero, denoted as SS = B1, which result in higher flow rates of blast furnace than the designed value. In the second stage, the flow rate of blast furnace gas decreases to meet the residence time requirement, denoted as SS = B2.

Fig. 11 shows the effects of fuel switching schemes on the inflowing flow rate, equivalent ratio and residence time. All the flow rates are normalized by defining the initial flow rate of coke oven gas as 1.0. The start time and end time of SS = A and SS = B1 are the 5th s and 15th s, and the start time and end time of SS = B2 are the 15th s and 20th s respectively. Subsequent simulations follow the same switch settings.

Fig. 11a and 11b show the inflowing flow rate changes for SS = A and SS = B. The flow rates of coke oven gas for both switching schemes change in the same way. But different switching schemes have dramatically different impacts on the flow rate of blast furnace gas. For SS = A, the flow rate of blast furnace gas is opposite to that of coke oven gas. For SS = B, the flow rate of blast furnace gas increases linearly from 0.0 to the peak point (Point K) in SS = B1, and decreases linearly from the peak point to 1.0 in SS = B2. The peak value of Point K (5.56) is the calorific value ratio of coke oven gas to blast furnace gas per unit volume.

Fig. 11c and 11d demonstrate the changes of inflowing equivalent

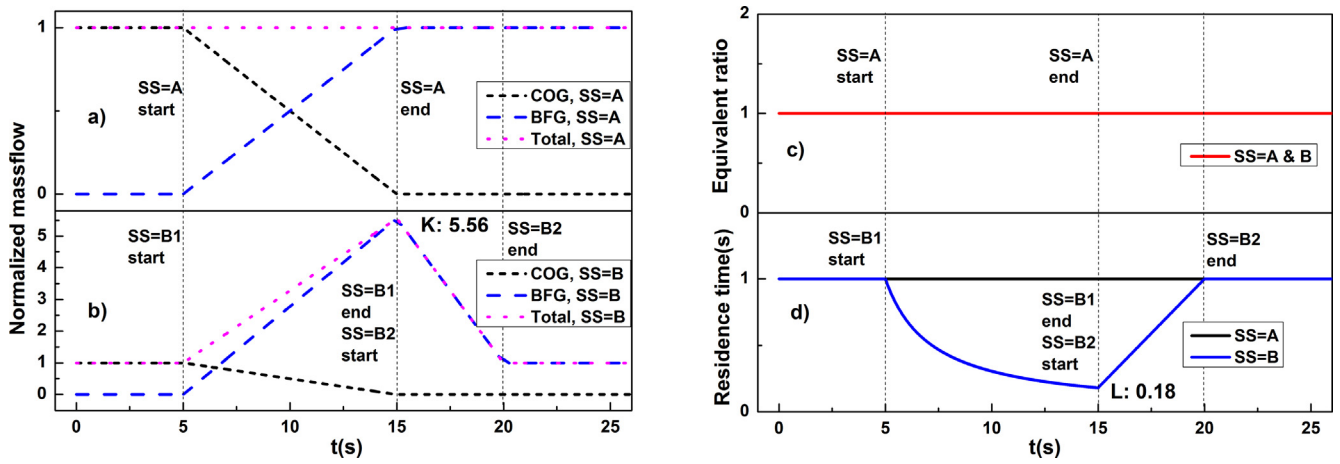

Fig. 11. Effects of switching schemes on the inflowing flow rate, equivalent ratio and residence time. (a) inflowing flow rate changes for SS = A; (b) inflowing flow rate changes for SS = B; (c) inflowing equivalent ratio changes for SS = A and B; (d) residence time changes for SS = A and B. Key: black dashed line, flow rate of coke oven gas; blue dashed line, flow rate of blast furnace gas; pink dotted line, flow rate of total gas; red solid line, equivalent ratio for SS = A and B; black solid line, residence time for SS = A; blue solid line, residence for with SS = B. (For interpretation of the references to colour in this figure legend, the reader is referred to the web version of this article.)

ratio and residence time with different fuel switching schemes. The inflowing equivalent ratio for both switching schemes stay constant during the whole process. For SS = A, the residence time stays constant. For SS = B, it decreases in a hyperbolic tend from 1.0 s to the lowest point (Point L) in SS = B1, and goes back to the original value (1.0 s) in SS = B2. The value of Point L (0.18) is the inverse of calorific value ratio of coke oven gas to blast furnace gas per unit volume.

The discussion presented above suggests that different fuel switching schemes will cause the same inflowing equivalent ratio, different inflowing flow rates and different residence times, and finally result in different combustion characteristics.

3.4.2. Combustion characteristics during fuel switching

The effects of fuel switching schemes and initial states on combustion characteristics are demonstrated in Fig. 12. For stable combustion initial state (SCIS), the temperature drops linearly from the initial temperature of coke oven gas (1296 K) to the final operating temperature of blast furnace gas (1106 K) for SS = A in Fig. 12a. By contrast, the temperature basically remains unchanged in SS = B1, and rapidly drops to the final combustion temperature of blast furnace gas in SS = B2, as shown in Fig. 12b.

For oscillating combustion initial state (OCIS), the mean temperature changes are the same as those with stable combustion initial state, as shown in Fig. 12c and 12d. This implies that combustion characteristics during fuel switching stage are mainly affected by fuel switching schemes but not by initial states. It is observed that fuel switching schemes have significantly different impacts on the attenuation process of the initial temperature oscillations. For SS = A, the initial temperature oscillations maintain at the beginning, and gradually decay to zero with the decrease of mean temperature. For SS = B, the initial temperature oscillations disappear rapidly at the very beginning of fuel switching. This suggests that scheme B has a stronger inhibitory effect on the initial temperature oscillations as the hydrogen content drops more rapidly. The attenuation processes of temperature oscillations can be seen in the enlarged view of Fig. 12c and 12d.

3.4.3. Effects of flow rate fluctuations on combustion characteristics during fuel switching

a) Operating condition analysis

Considering the conditions of industrial practice, flow rate fluctuation is a common phenomenon. Flow rate fluctuation of hot air heater (denoted as FT = F) only affects the flow rate of blast furnace gas. The flow rates of coke oven gas and air remain unchanged. The frequency of field flow rate fluctuations is 1 Hz. Cases without fluctuation are denoted as FT = 0.

Fig. 13 demonstrates the effects of flow rate fluctuations and fuel switching schemes on the inflowing flow rate and equivalent ratio. As shown, the flow rate and equivalent ratio of coke oven gas does not fluctuate. The flow rates of blast furnace gas and total gas fluctuate from the start time of fuel switching with increasing amplitudes until

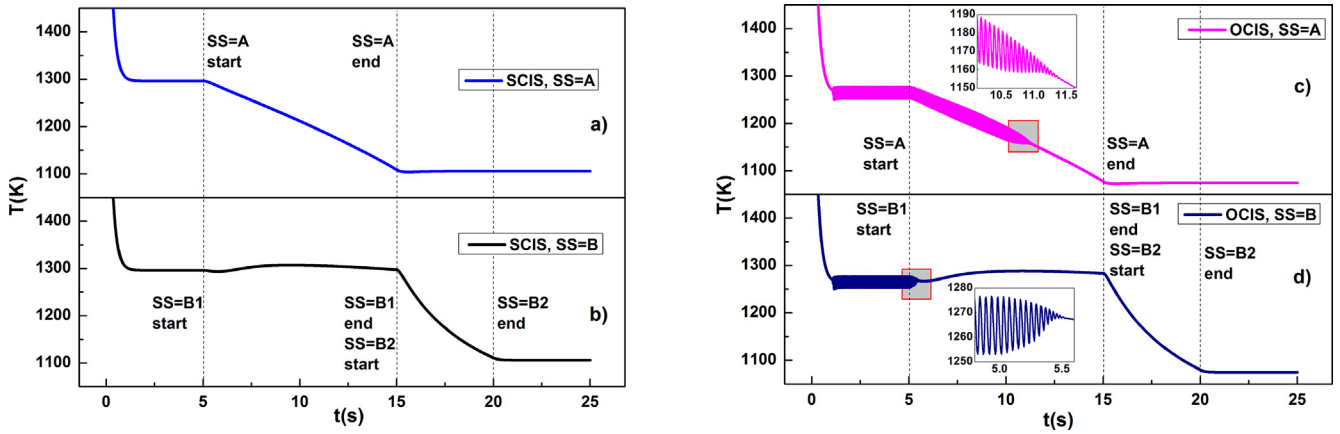

Fig. 12. Effects of fuel switching schemes and initial states on combustion characteristics. (a) SCIS, SS = A; (b) SCIS, SS = B; (c) OCIS, SS = A; (d) OCIS, SS = B.

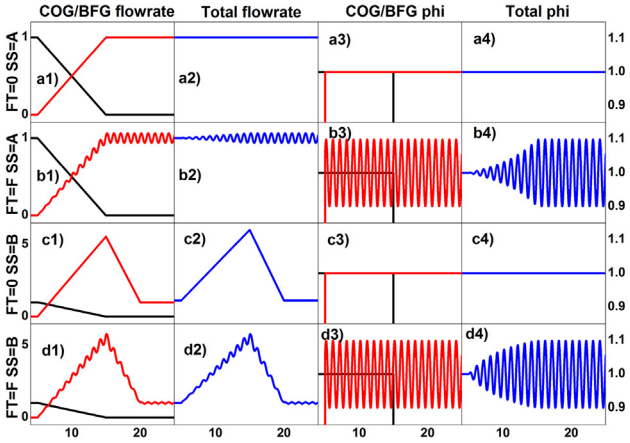

Fig. 13. Effects of flow rate fluctuations and fuel switching schemes on the inflowing flow rate and equivalent ratio. (a) FT = 0, SS = A; (b) FT = F, SS = A; (c) FT = 0, SS = B; (d) FT = F, SS = B. Keys: Column 1, flow rate changes of coke oven gas and blast furnace gas; Column 2, flow rate changes of total gas; Column 3, equivalent ratio changes of coke oven gas and blast furnace gas; Column 4, equivalent ratio changes of total gas; Black solid line, coke oven gas; Red solid line, blast furnace gas; Blue solid line, total gas. (For interpretation of the references to colour in this figure legend, the reader is referred to the web version of this article.)

saturation. The equivalent ratio of blast furnace gas fluctuates with equal period and amplitude, and the equivalent ratio of total gas fluctuates with increasing amplitude until saturation. The mean flow rate and equivalent ratio for FT = F are consistent with those for FT = 0 when using the same fuel switching scheme.

b) Effects of initial states coupling flow rate fluctuations

The effects of initial states and flow rate fluctuations on combustion characteristics are demonstrated in Fig. 14 for the cases (OCIS, FT = 0; OCIS, FT = F and SCIS, FT = F) with the same fluctuation range of Ra = ± 10%. By comparing Fig. 14b with 14a, the initial temperature fluctuations in Fig. 14b decay more rapidly than that in Fig. 14a, where no flow rate fluctuation is involved. It suggests that flow rate fluctuation changes the combustion characteristics dramatically during the fuel switching stage.

In Fig. 14b, the temperature fluctuations are periodically clustered, as seen in the enlarged view. Within one cluster, the fluctuation period is constant, and the amplitude gradually attenuates after a sudden increase at the initial moment. Between clusters, the amplitudes of temperature fluctuations first increase and then decrease. In Fig. 14c, the initial temperature fluctuations disappear rapidly, and the following

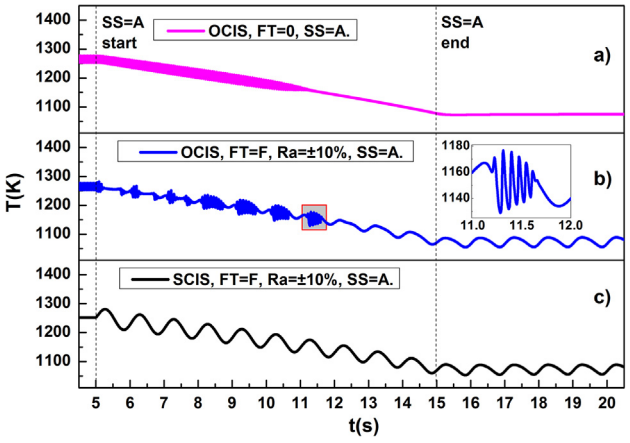

Fig. 14. Effects of initial states and flow rate fluctuations on combustion characteristics with the same fluctuation amplitude of Ratio = ± 10%. (a) OCIS, FT = 0; (b) OCIS, FT = F; (c) SCIS, FT = F.

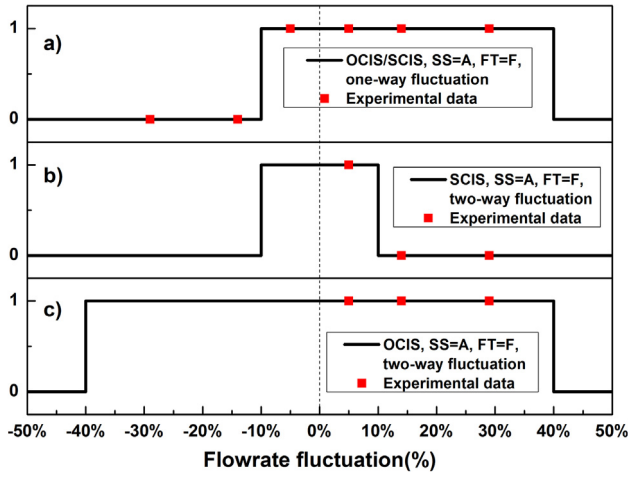

Fig. 15. Effects of initial states on the tolerance range of flow rate fluctuations. (a) OCIS/SCIS, FT = F, one-way fluctuations; (b) SCIS, FT = F, two-way fluctuations; (c) SCIS, FT = F, two-way fluctuations. Key: red squares, experimental data; 1, burnt; 0, unburnt. (For interpretation of the references to colour in this figure legend, the reader is referred to the web version of this article.)

temperature fluctuations are periodic with equal period and amplitude. After fuel switching, the temperature fluctuations in Fig. 14b and 14c are the same. By comparing Fig. 14b with 14c, it suggests that different initial states result in different combustion characteristics during the fuel switching stage. Affected by the initial oscillating combustion before fuel switching, the combustion process is more complicated during the switching process in Fig. 14b.

The effects of initial states on the tolerance range of flow rate fluctuations are shown in Fig. 15. As shown in Fig. 15a, SCIS and OCIS cases have the same tolerance range of the one-way flow rate fluctuations, and the tolerance limits of decreasing flow rate and increasing flow rate are −10% and + 40% respectively. This suggests that the system has a stronger adaptability to the one-way fluctuations of increasing flow rate. By comparing Fig. 15b with 15c, the tolerance ranges of the two-way flow rate fluctuations for OCIS case (± 40%) are much larger than that for SCIS case (± 10%).

The discussion presented above suggests that OCIS case has a stronger adaptability to flow rate fluctuations than SCIS case. The tolerance range of flow rate fluctuations in the hot air heater are tested under different fluctuation amplitudes from 5% to 29%. The experiment data are shown by red squares in Fig. 15. As shown, the model results agree well with the experimental data. Therefore OCIS is the optimal initial condition for fuel switching, considering it can broaden the tolerance range of flow rate fluctuations to improve operation stability of the system.

c) Effects of fuel switching schemes coupling flow rate fluctuations

Fig. 16 demonstrates the effects of fuel switching schemes on combustion characteristics with the same fluctuation range of Ra = ± 10% and the same oscillating combustion initial state (OCIS). By comparing Fig. 16a with 16b, the temperature oscillates periodically in Fig. 16b due to the effect of flow rate fluctuations. By comparing Fig. 16b with 16c, the combustion characteristics are simpler in Fig. 16b than in Fig. 16c due to the rapid decrease of hydrogen content at the beginning of fuel switching process, and no periodically clustered temperature oscillations occur in Fig. 16b.

The effects of fuel switching schemes on the tolerance range of flow rate fluctuations with the same oscillating combustion initial state are shown in Fig. 17. As shown, the tolerance limits of one-way fluctuations of decreasing and increasing flow rate broaden from −10%, 40% for SS = A to −10%, 60% for SS = B. The tolerance limit of two-way fluctuations broadens from ± 40% for SS = A to ± 50% for SS = B. This suggests that fuel switching scheme B has a much stronger

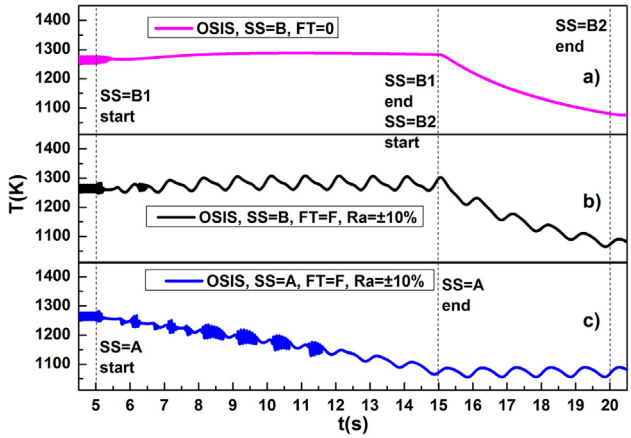

Fig. 16. Effects of fuel switching schemes and flow rate fluctuations on combustion characteristics with the same fluctuation range of Ra = ± 10% and the same oscillating combustion initial state. (a) FT = 0, SS = B; (b) FT = F, SS = B; (c) FT = F, SS = A.

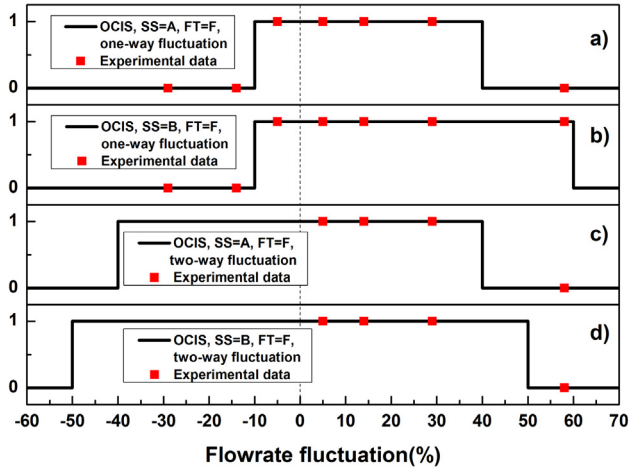

Fig. 17. Effects of fuel switching schemes on the tolerance range of flow rate fluctuation with the same oscillating combustion initial state. (a) SS = A, FT = F, one-way fluctuations; (b) SS = B, FT = F, one-way fluctuations; (C) SS = A, FT = F, two-way fluctuations; (d) SS = B, FT = F, two-way fluctuations. Key: red squares, experimental data; 1, burnt; 0, unburnt. (For interpretation of the references to colour in this figure legend, the reader is referred to the web version of this article.)

adaptability to flow fluctuations than fuel switching scheme A. The field test data for different fluctuation amplitudes of 5%, 14% and 29% are shown by red squares in Fig. 17, and validate the simulation results. Therefore the optimal fuel switching scheme is fuel switching scheme B, considering it can broaden the tolerance range of flow rate fluctuations to improve operation stability of the system.

4. Conclusions

An unsteady PSR combustion model together with chemical explosive mode analysis has been established to analyze the combustion stability of burning blast furnace gas and coke oven gas. The complex oscillatory dynamics has been successfully reproduced. Results show the differences in the combustion stabilities. For blast furnace gas, a critical ambient temperature needs to be maintained for stable combustion due to its calorific. Temperature, H and R36 ($H+O_2+N_2HO_2+N_2$) are dominant at the inflection point of extinction. For coke oven gas, temperature may oscillate in specific ambient temperature ranges. Temperature, O_2 and R35 ($H+O_2+H_2OHO_2+H_2O$) are dominant in the oscillating combustion within one single period.

It is further found that gas composition and equivalence ratio have pronounced effects on combustion instability. Blast furnace gas with higher hydrogen content can dramatically low the critical ambient temperature: when hydrogen content increases from 1% to 5%, the critical ambient temperature that can sustain burnt state decreases from 840 K to 790 K. Coke oven gas with high hydrogen content or low carbon monoxide content can be burnt more stable and the ambient temperature range for oscillating combustion narrows. It is further shown that the fraction of blast furnace gas in the blended mixture should exceed a large critical value, i.e., around 80%, to inhibit oscillating combustion. Slight fuel lean combustion of coke oven gas is beneficial to inhibit oscillating combustion.

During fuel switching stage, the combustion characteristics are mainly affected by fuel switching schemes but not by initial states. Fuel switching scheme B has a stronger ability to suppress the initial temperature oscillations than scheme A. Compared to stable combustion initial state (SCIS), oscillating combustion initial state (OCIS) increases the tolerance range of flow rate fluctuations by 30%. The tolerance range for fuel switching scheme B is 10% wider than that for scheme A. The optimal initial state and fuel switching scheme are oscillating combustion initial state (OCIS) and fuel switching scheme B (SS = B).

CRediT authorship contribution statement

Long Zhang: Conceptualization, Methodology, Writing - original draft. **Wenwen Xie:** Writing - review & editing. **Zhuyin Ren:** Supervision.

Declaration of Competing Interest

The authors declare that they have no known competing financial interests or personal relationships that could have appeared to influence the work reported in this paper.

Acknowledgements

The work is supported by National Natural Science Foundation of China 91841302

References

[1] Johansson MT, Soederstrom M. Options for the Swedish steel industry - Energy efficiency measures and fuel conversion. Energy 2011;36(1):191–8.
[2] Rosado DJ, Chávez SB, Gutierrez JA, et al. Energetic analysis of reheating furnaces in the combustion of coke oven gas, Linz-Donawitz gas and blast furnace gas in the steel industry. Appl Therm Eng 2020;169:114905–20.
[3] Caillat S. Burners in the steel industry: utilization of by-product combustion gases in reheating furnaces and annealing lines. Energy Procedia 2017;120:20–7.
[4] Razzaq R, Li C, Zhang S. Coke oven gas: Availability, properties, purification, and utilization in China. Fuel 2013;113:287–99.
[5] Li Z, Yi Q, Zhang Y, et al. Numerical study and design strategy for a low emission coke oven system using oxy-fuel combustion of coke oven gas. J Cleaner Prod 2020;252:119656–71.
[6] Ba A, Cessou A, Marcano N, et al. Oxyfuel combustion and reactants preheating to enhance turbulent flame stabilization of low calorific blast furnace gas. Fuel 2019;242:211–21.
[7] Nguyen P, Ghazal G, Piñera V, et al. Modelling of flameless oxy-fuel combustion with emphasis on radiative heat transfer for low calorific value blast furnace gas. Energy Procedia 2017;120:492–9.
[8] Ilbas M, Bektas A, Karyeyen S. A new burner for oxy-fuel combustion of hydrogen containing low-calorific value syngases: An experimental and numerical study. Fuel 2019;256:115990–6004.
[9] Zhang K, Jiang X. Uncertainty quantification of fuel variability effects on high hydrogen content syngas combustion. Fuel 2019;257:116111–23.
[10] Yilmaz H, Cam O, Yilmaz I. A comparison study on combustion and emission characteristics of actual synthetic gas mixtures. Fuel 2020;263:116712–28.
[11] Karyeyen S, Ilbas M. Experimental and numerical analysis of turbulent premixed combustion of low calorific value coal gases in a generated premixed burner. Fuel 2018;220:586–98.
[12] Zhou Q, Cheung CS, Leung CW, et al. Effects of fuel composition and initial pressure on laminar flame speed of $H_2/CO/CH_4$ bio-syngas. Fuel 2019;238:149–58.
[13] Lee HC, Mohamad AA, Jiang LY. A detailed chemical kinetics for the combustion of $H_2/CO/CH_4/CO_2$ fuel mixtures. Fuel 2017;193:294–307.

[14] Yongliang Xie Na Lv Qizhang Li Jinhua Wang Effects of CO addition on laminar flame characteristics and chemical reactions of H2 and CH4 in oxy-fuel (O2/CO2) atmosphere Int J Hydrogen Energy 2019 10.1016/j.ijhydene.2019.10.138.
[15] Ziani L, Chaker A, Chetehouna K, et al. Numerical simulations of non-premixed turbulent combustion of CH_4/H_2 mixtures using the PDF approach. Int J Hydrogen Energy 2013;38(20):8597–603.
[16] Mardani A. Optimization of the Eddy Dissipation Concept (EDC) model for turbulence-chemistry interactions under hot diluted combustion of CH_4/H_2. Fuel 2017;191:114–29.
[17] Zohra KF, Mounir A, Salah C. Numerical simulation of CH_4/H_2/AIR non-premixed flame stabilized by a bluff body. Energy Procedia 2017;139:530–6.
[18] Fischer M, Jiang X. A chemical kinetic modelling study of the combustion of $CH_4/CO/H_2/CO_2$ fuel mixtures. Combust Flame 2016;167:274–93.
[19] Choi M, Park Y, Li X, et al. Study on flame structures and emission characteristics according to various swirl combinations and fuel compositions in a CH_4/H_2/CO syngas swirl-stabilized combustor. Fuel 2019;253:887–903.
[20] Cheng TS, Chang YC, Chao YC, et al. An experimental and numerical study on characteristics of laminar premixed $H_2/CO/CH_4$/air flames. Int J Hydrogen Energy 2011;36(20):13207–17.
[21] Liu C, Song H, Zhang P, et al. A rapid compression machine study of autoignition, spark-ignition and flame propagation characteristics of $H_2/CH_4/CO$/air mixtures. Combust Flame 2018;188:150–61.
[22] Cho KW, Han K, Lee YK, et al. Premixed combustion of coke oven gas in a metallic fibre mat. Fuel 2001;80(7):1033–6.
[23] R. Ortiz-Imedio A. Ortiz J.C. Urroz P.M. Diéguez D. Gorri L.M. Gandía I. Ortiz Comparative performance of coke oven gas, hydrogen and methane in a spark ignition engine Int J Hydrogen Energy 2020 10.1016/j.ijhydene.2019.12.165.
[24] H. Wang H. Zhou Z. Ren et al. Proceedings of the Combustion Institute 2019 4487 4495.
[25] Victor CP, Diego CR, Nguyen PD, et al. Blast furnace gas based combustion systems in steel reheating furnaces. Energy Procedia 2017;120:357–64.
[26] He J, Chen Z, Jiang X, et al. Combustion characteristics of blast furnace gas in porous media burner. Appl Therm Eng 2019;160:113970–7.
[27] Smith G P, Golden D M, Frenklach M, et al. http://www.me.berkeley.edu/gri_mech/.
[28] Ren Z, Pope SB. Reduced description of complex dynamics in reactive systems. J Phys Chem A 2007;111(34):8464–74.
[29] Shan R, Lu TF. Ignition and extinction in perfectly stirred reactors with detailed chemistry. Combust Flame 2012;159(6):2069–76.
[30] Snegirev AY. Perfectly stirred reactor model to evaluate extinction of diffusion flame. Combust Flame 2015;162(10):3622–31.
[31] Sabia P, Joannon MD, Fierro S, et al. Hydrogen-enriched methane MILD combustion in a well stirred reactor. Exp Therm Fluid Sci 2007;31(5):469–75.
[32] Chen Z, Reddy VM, Ruan S, et al. Simulation of MILD combustion using Perfectly Stirred Reactor model. Proc Combust Inst 2017;36(3):4279–86.
[33] Caracotsios M, Stewart WE. Sensitivity analysis of initial value problems with mixed odes and algebraic equations. Comput Chem Eng 1985;9(4):359–65.
[34] Lu TF, Yoo CS, Chen JH, et al. Three-dimensional direct numerical simulation of a turbulent lifted hydrogen jet flame in heated coflow: a chemical explosive mode analysis. J Fluid Mech 2010;652:45–64.
[35] Wu W, Piao Y, Xie Q, et al. Flame Diagnostics with a Conservative Representation of Chemical Explosive Mode Analysis. AIAA Journal 2019;57(4):1355–63.
[36] Luo Z, Yoo CS, Richardson ES, et al. Chemical explosive mode analysis for a turbulent lifted ethylene jet flame in highly-heated coflow. Combust Flame 2012;159(1):265–74.